

Thousands of shallow, relict gullies indicate thermo-erosion on the sandy uplands of northern Lower Michigan during the Late Pleistocene

Christopher J. Baish ^{a,*}, Alanna Post ^a, Ashton M. Shortridge ^a, Randall J. Schaetzl ^a, Parker Hopkins ^b, Anthony Bowman ^a, Isabella Rabac ^c, Bernard Frantz ^d, Andrew O. Finley ^b

^a Department of Geography, Environment, and Spatial Sciences, Michigan State University, East Lansing, MI 48823, United States of America

^b Department of Forestry, Michigan State University, East Lansing, MI 48823, United States of America

^c Department of Community Sustainability, Michigan State University, East Lansing, MI 48823, United States of America

^d Department of Plant, Soil, and Microbial Sciences, Michigan State University, East Lansing, MI 48823, United States of America

ARTICLE INFO

Keywords:

Permafrost
Thermo-erosion
Active-layer
Longitudinal profile
Water tracks

ABSTRACT

We build on previous work which explained the origin of myriad gullies and incised channels on the dry, sandy uplands of northern Lower Michigan by invoking widespread permafrost. Indicators of permafrost (ice-wedge casts and patterned ground) are known from many sites across the region. Our study area, within an extensive reentrant of the retreating Laurentide Ice Sheet, had been particularly well positioned, geographically, for permafrost. Our goal was to characterize the geomorphic characteristics of the gullies on 72 large ridges, to address the hypothesis that they had formed in association with permafrost. Across the study area, thousands of dry, narrow channels and gullies occur in dense networks, typically with channels aligned directly downslope, in parallel drainage patterns. Most of the gullies exhibit only a minimal amount of incision (ca. 2–3 m), a nearly straight longitudinal profile, and lack a clear depositional fan at their mouth. Even where small fans are present, they are subtle and exhibit little down-fan textural sorting, as would be present in larger, more mature fluvial systems. Gully morphologies did not exhibit strong morphological differences as a function of aspect, as we would have expected for an erosional, periglacial system forming on fairly steep slopes. Nonetheless, in these sandy/gravelly sediments, we could find no other scenario that would have allowed for runoff and gully formation, except ice-rich permafrost that limited infiltration and promoted saturation of the active layer, and eventually, runoff. We conclude that the gullies formed via thermo-erosion into ice-rich permafrost, involving mostly fluvial processes but also some slope failure. Even though thermo-erosion can rapidly form deep gullies, our study area has mainly weak gully forms, perhaps because: (1) permafrost existed here only briefly, (2) the landscape was so cold and the permafrost so ice-rich that runoff was rare, (3) the permafrost on the sandy slopes remained somewhat permeable, limiting runoff, and/or (4) the paleoclimate was so dry that little water was available for sediment transport. We could find no evidence that the gullies developed within preexisting polygonal networks, as is happening today in polar regions under a warming climate. Thus, our study has implications for areas of the Arctic and Antarctic that are, today, experiencing rapid hydrological changes.

1. Introduction

Fluvial erosion can sometimes form deep, relatively permanent, ephemeral channels, which (depending on their size) are often referred to as rills or gullies. Channels like these have no base flow and are often dry. Most gullies begin at a source alcove, continue downstream along a transportation channel, and end in a fan or similar depositional feature (Conway et al., 2018). Taken to extremes, deep, narrow, actively

forming gullies can be difficult to traverse, or in areas of cropland, to remove with conventional tillage equipment (Poesen et al., 2003; Goudie, 2004; Zgobicki et al., 2019; Thwaites et al., 2022). Typically, gullies form as surface runoff exceeds the critical shear stress required for particle detachment, leading to channel initiation and propagation (deepening and extension). Thus, gully erosion is a unique type of geomorphic threshold phenomenon that reflects slope instability, either currently or in the past (Patton and Schumm, 1975; Schumm, 1979;

* Corresponding author.

E-mail address: baishchr@msu.edu (C.J. Baish).

Vandaele et al., 1996; Poesen et al., 2003; Belayneh et al., 2024).

Considerable research has been dedicated to understanding how gullies (of all kinds) form and the drivers for gully-like erosion (Castillo and Gómez, 2016; Valentin et al., 2005; Conway et al., 2015). The gully formation process can be affected by a wide range of factors, including flow hydraulics, precipitation intensity and duration, topography, land cover, and the underlying sediment, particularly its permeability (Poesen et al., 2003; Valentin et al., 2005; Zachar, 2011; Torri and Poesen, 2014). Much of this work has necessarily focused on active gully systems, often driven by recent land use changes. For example, agricultural, forestry, and construction activities often alter the local hydrology and initiate gully formation (Sidorchuk, 1999; Castillo and Gómez, 2016). With the exception of work on other planets (see below), comparatively less effort has been applied to inactive, or relict, gully forms that occur on surfaces where conditions are currently unfavorable for gully erosion. Indeed, most studies of relict gullies (on Earth) have been limited to areas where hillslope instability is linked to historic conversion of land to cultivation or grazing practices (Valentin et al., 2005). These types of relict gully systems have been studied in Europe (Wilkinson, 2003; Zglobicki et al., 2019), Africa (Tebebu et al., 2010; Costanzo et al., 2022), Asia (Sidorchuk and Golosov, 2003; Avni, 2005; Ponomarenko et al., 2020), and North America (Spell and Johnson, 2019).

Few studies exist on relict gullies (on Earth) at sites minimally influenced by human activities, and most of this work has been focused in the northern mid-latitudes, e.g., Europe (Langoth and Sanders, 1985; Soms, 2011), Asia (Panin et al., 2009), and North America (Schaetzl, 2008). In these studies, geomorphic evidence and/or age control often point to a defined (sometimes short) interval of hillslope instability and incision, well before human occupation and any associated land use changes. Because each such location would have experienced relatively mild Holocene climatic conditions with persistent vegetative cover, it was concluded that incision must have occurred during the Late Pleistocene, and thus, was likely periglacial in origin and driven by reduced permeabilities caused by impermeable or slowly permeable permafrost (Bogaart et al., 2003). Such settings and conditions (ice-marginal areas during the Late Pleistocene) have also been invoked to explain regional-scale hillslope instability and the formation of (currently) dry valleys in Wisconsin, USA (Leigh and Knox, 1994; Jacobs et al., 1997; Mason and Knox, 1997; Mason, 2015) and Europe (Klatkowa, 1967). In short, the presence of permafrost, which can and often does lead to periodic saturation within the active layer, may force Hortonian overland flow to occur on sloping surfaces, potentially leading to spring seeps and gully formation (Fig. 1).

Gully erosion is common on modern periglacial landscapes of the Arctic (Perreault et al., 2017; Sidorchuk, 2020; Nicu et al., 2022) and Antarctic (Levy, 2015; Dickson et al., 2019; Hauber et al., 2019). Indeed, these landscapes are, today, becoming increasingly vulnerable to gully and gully-like erosion, due to thawing permafrost and thickening active layers (Brown and Mote, 2009; Rowland et al., 2010; Godin et al., 2014; Del Vecchio et al., 2023). Enhanced gully formation in these locations is often due to thermo-erosion within the saturated active layer (Fig. 1). If the upper layer of permafrost is ice-rich, as is common, thermo-erosion can release large amounts of water to the active layer, enhancing saturation and initiating a positive feedback loop. These areas of saturated water in the active layer are often referred to as water tracks or dells (Del Vecchio et al., 2024). Recently, a large body of literature focusing on the sensitivity of hillslope systems in periglacial environments has emerged (Biskaborn et al., 2019). This work broadly highlights the need for studies of gully formation in other areas, particularly those which may have experienced periglacial conditions in the past. We argue that such research should focus on cataloguing and characterizing relict gullies, with the goal of better understanding hillslope responses to past (periglacial) environments.

Northern Lower Michigan (USA) is rife with thousands of gullies and incisional features, all apparently relict and currently stable (see below).

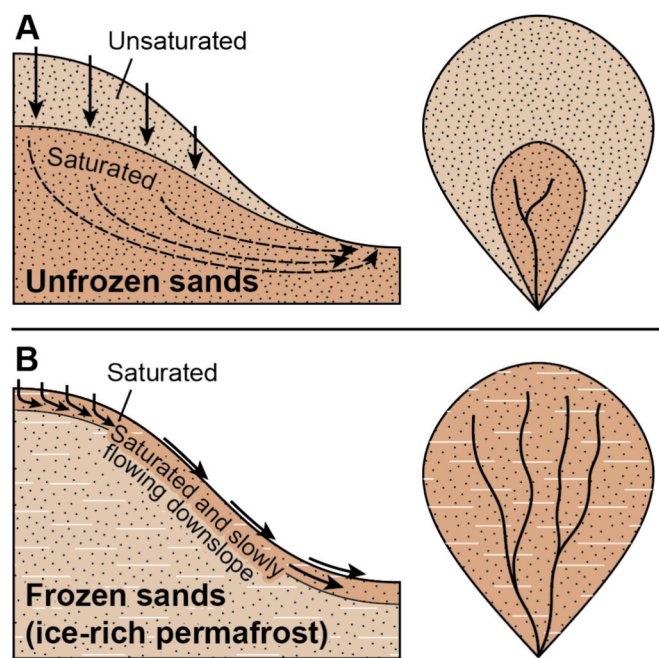


Fig. 1. Illustration of the effect of impermeable permafrost on hillslope hydrology and drainage networks in sandy sediments. A. Unfrozen conditions, which allow for nearly unimpeded infiltration. B. The same landscape with permafrost, forcing water to flow downslope within the saturated active layer. After Bogaart et al. (2003).

The gullies occur as dense, linear (and often parallel) networks that extend down the flanks of sandy/gravelly, ridges (Fig. 2). The valleys and ravines that dominate these side slopes defy conventional notions of gully formation, as they occupy densely vegetated surfaces that are underlain by highly permeable, coarse-textured sediment which only rarely exhibits any type of runoff (Schaetzl et al., 2021a). Schaetzl (2001) went so far as to conclude that these gullies could only have formed during a former interval of frozen ground, when surface permeabilities were much lower. Thus, the gullies and other incised channels in our study area have potential significance as paleoenvironmental proxies, and are therefore worthy of focused research.

Our study involves a detailed geomorphic examination and interpretation of a subset of the many gullies that occur throughout the northern Lower Peninsula of Michigan. Despite focusing on a subset of gullies from northern Lower Michigan, our approach involves mapping and characterizing thousands of gully forms. We then use these data to interpret the factors that may have controlled gully formation processes, thereby providing a window into the paleoenvironment of the study area, and perhaps the broader region, in the postglacial period.

In our study, we utilized various geomorphological datasets and tools, reinforced with geostatistics, to map and characterize 8800 gully networks on a series of large, sandy ridges that collectively span almost 3100km². Additionally, we examined the physical characteristics of a select few, well-defined gully systems to provide insight into their sediments and sediment transport processes. We couched our findings around the hypothesis that the gullies document an interval when periglacial conditions, i.e., permafrost, dominated this region during the postglacial period, leading to hillslope instability and erosion on otherwise stable uplands (Schaetzl, 2008). Our large dataset and rigorous statistical approach represent a comprehensive characterization of gullied slopes not previously attempted, and may serve as a framework for future research on gully networks – both relict and active – across regional scales.

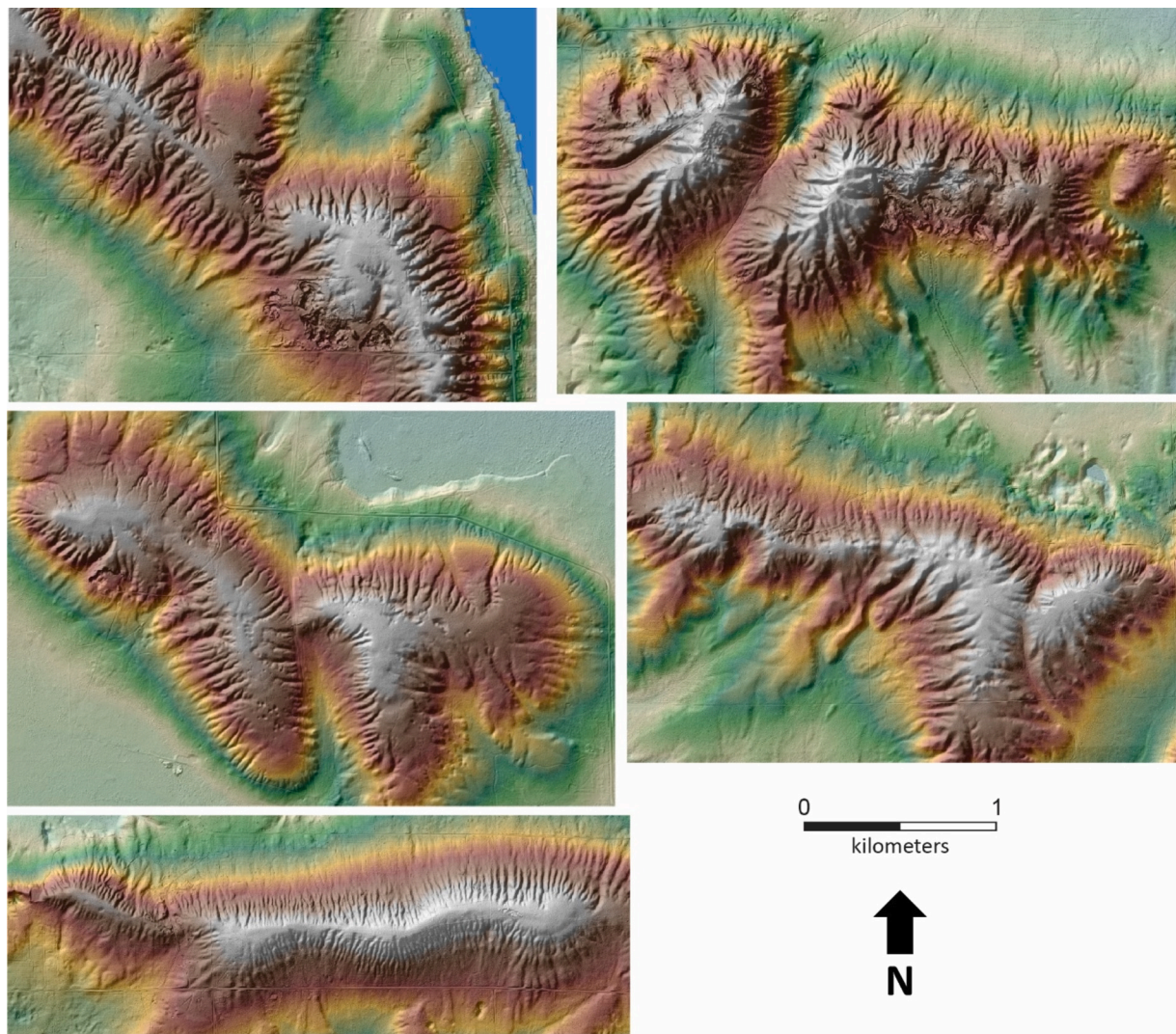


Fig. 2. Examples of ridge sites within our study area that typify the gully forms across the wider region. Illustrations were derived using a hillshade and color DEM derived from 1-m LiDAR data. All sites are shown at a similar scale.

2. Regional setting and paleoclimate

Our initial mapping efforts focused on gullied/incised features across all of northern Lower Michigan. Gullies are so (seemingly) ubiquitous across this region that our initial data set contained >250,000 such “gullies”. Thus, we restricted the study area to a series of large, sandy ridges in the central Lower Peninsula, where gullies are particularly well-developed (Fig. 3). Restricting the study area allowed us to control for variations in substrate lithology, as well as geomorphic, climatic, and land-use histories. Physiographically, the study area is centered on the Houghton Lake Basin, part of the Houghton Lake Sandy Flats and Ridges province (Schaetzl et al., 2013); three of the northern-most ridges are in the Grayling Fingers province (Fig. 3). This area largely owes its geomorphology to the activity of the Mackinac Lobe of the Laurentide Ice Sheet (Burgis, 1977; Schaetzl, 2001; Schaetzl and Weisenborn, 2004; Schaetzl et al., 2017).

The seven prominent ridges that span the study area are various types of ice-contact fans and kame deltas of the Mackinac Glacial Lobe, formed both subaqueously and subaerially. The ridges are almost entirely composed of stratified and well-sorted sand and gravel, as shown on water well logs and at exposures in gravel and borrow pits. Local soil maps describe almost all of the soils on the ridges as being well-drained or drier; water tables are often in excess of 3–10+ m deep

(Frederick, 1985; Werlein, 1998; Tardy, 2005). Most ridges are currently forested, due to the steep slopes and dry, sandy soils, i.e., agriculture is not a feasible option. We focused on 74 discrete sections of the seven ice-contact ridges for our work, each of which contained an isolated upland with numerous gullies (Figs. 2, 3).

Knowledge of the postglacial paleoclimate of the study area - and the broader region - is central to our analysis. Southern Michigan was covered by the Laurentide Ice Sheet during Marine Isotope Stage 2 (Leverett and Taylor, 1915; Dworkin et al., 1985; Johnson et al., 1997; Larson and Kincare, 2009; Dalton et al., 2022). The retreat of the ice sheet in the midwestern US was episodic and asynchronous, but generally started between ca. 29 and 21 ka (Carson et al., 2012; Heath et al., 2018), and in some places, even later (Attig et al., 2011). Important to our research is a region-wide readvance of the ice sheet - the Port Huron readvance – onto the Lower Peninsula at ca. 15.2 ka (Blewett et al., 1993; Larson and Kincare, 2009). At the time of the Port Huron readvance, the Houghton Lake Basin would have been within a large reentrant of the ice sheet (Fig. 4). Researchers that have studied the paleoclimate of the Driftless Area of southwestern Wisconsin, which was also similarly bounded by ice (the Des Moines, Chippewa, and Green Bay Lobes) during the Late Pleistocene, described the landscape at this time as being “up in the refrigerator” (Mason, 2015; Carson et al., 2019). Abundant evidence exists for permafrost across the Driftless Area during

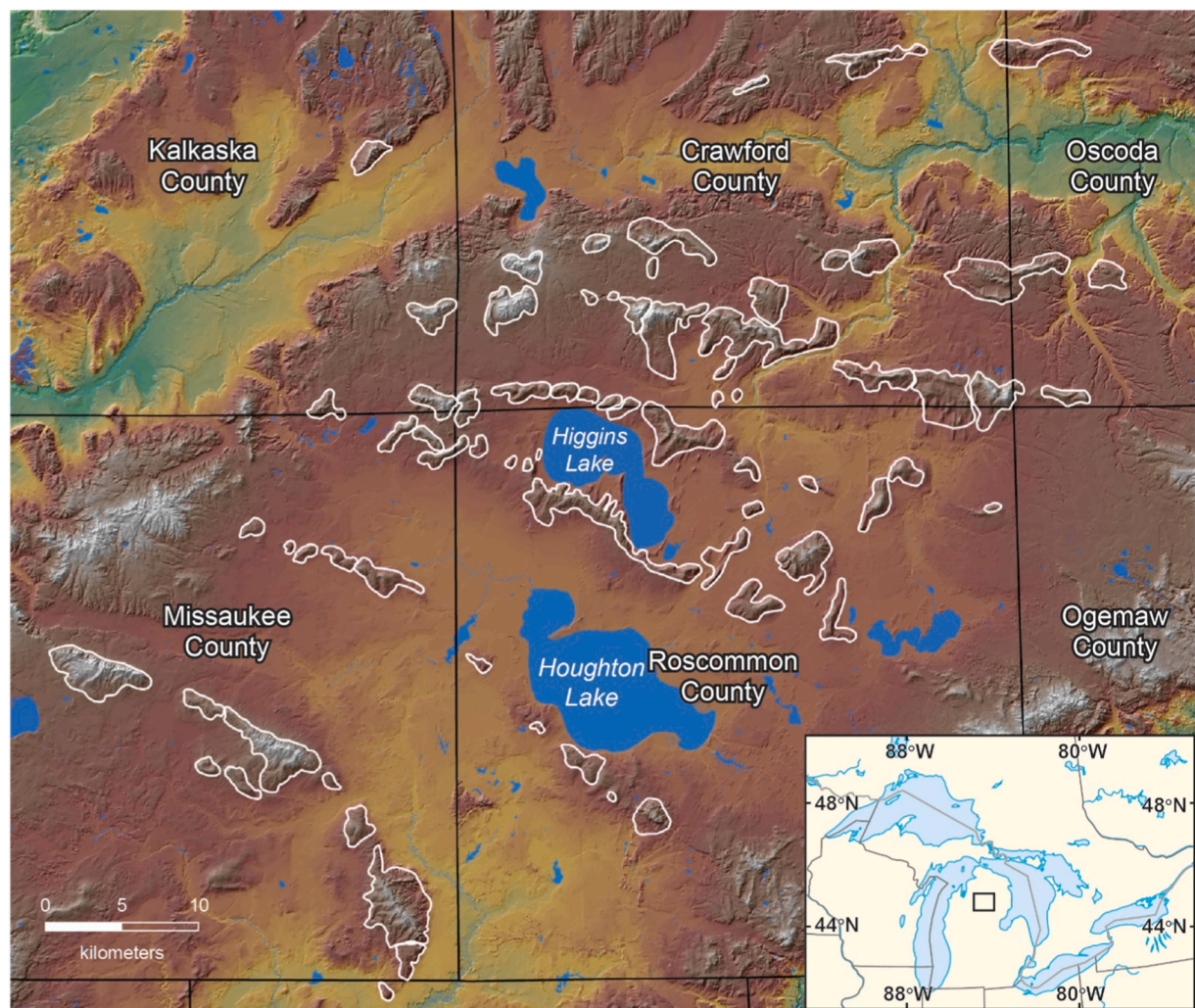


Fig. 3. The topography of the study area, showing the 72 ridge polygons (circled in white), whose gullies were the focus of our work.

this interval (Holmes and Syverson, 1997; Clayton et al., 2001; Batchelor et al., 2019; Schaetzl et al., 2021). Our study area was up in a similar “refrigerator” during the Port Huron advance (Fig. 4). At this time, no part of the study area would have been >45 km from the ice margin, and thus, might have been subjected to strong, cold, katabatic winds (Heinemann, 1999; Schaetzl and Attig, 2013). An even colder paleogeographic setup may also have existed for more than a millennium prior to that, while the Mackinac Lobe was retreating from the region and the ice margin was, in places, much closer to some of the ridges under study here.

As in Wisconsin, abundant evidence exists for permafrost in southern Michigan (Fig. 4). We recently identified several well-formed ice-wedge casts in a borrow pit in one of the ridges in the Houghton Lake Basin (unpublished data). Schaetzl (2008) used geomorphic and sedimentologic data to infer a period of enhanced runoff in the Grayling Fingers, just north of our study area. He concluded that runoff could only have occurred here (again, on sandy soils) due to permafrost. Lusch et al. (2009) identified extensive areas of patterned ground in the Saginaw Lowlands, 50–125 km south and east of our study area. These polygons would have formed slightly after the Port Huron Advance, pointing to the persistence of permafrost, even in areas considerably south of the study area, during the deglacial period.

Therefore, we began this study with the hypothesis that the gullies in the sandy ridges of Houghton Lake Basin were driven by runoff from frozen ground, i.e., with ice-rich permafrost. Similar situations occur today in the Arctic and Antarctic, and are documented for parts of Mars,

often where permafrost or an interval of enhanced runoff has been assumed to have occurred (McKnight et al., 1999; Malin and Edgett, 2000; Levy, 2015).

3. Materials and methods

Our study was carried out by a team of students, during a graduate-level seminar course under the guidance of two faculty members. This type of research structure provided for many opportunities to repeatedly inspect the data sets (a measure of quality control); at each phase of the project, different students examined and evaluated the data in a GIS. Having used this approach in the past, e.g., Hupy et al. (2005), Vader et al. (2012), Schaetzl et al. (2013, 2020), we knew the utility of team research efforts. Because of the large size of our data sets, utilizing a group of students enhanced our overall data quality and development effort.

3.1. Digital mapping of incisional features

Gullies and other incised channels are ubiquitous on ridges in the study area (Fig. 2). Our first goal, to map the gullies, began by delineating the mouth of each gully form, i.e., the point where the gully transitions (downstream) to a surface that lacks a channel. To accomplish this, we first downloaded 1-m LiDAR terrain datasets for the study area from the U.S. Geological Survey 3D Elevation Program and mosaicked them into a continuous raster file. To make data handling

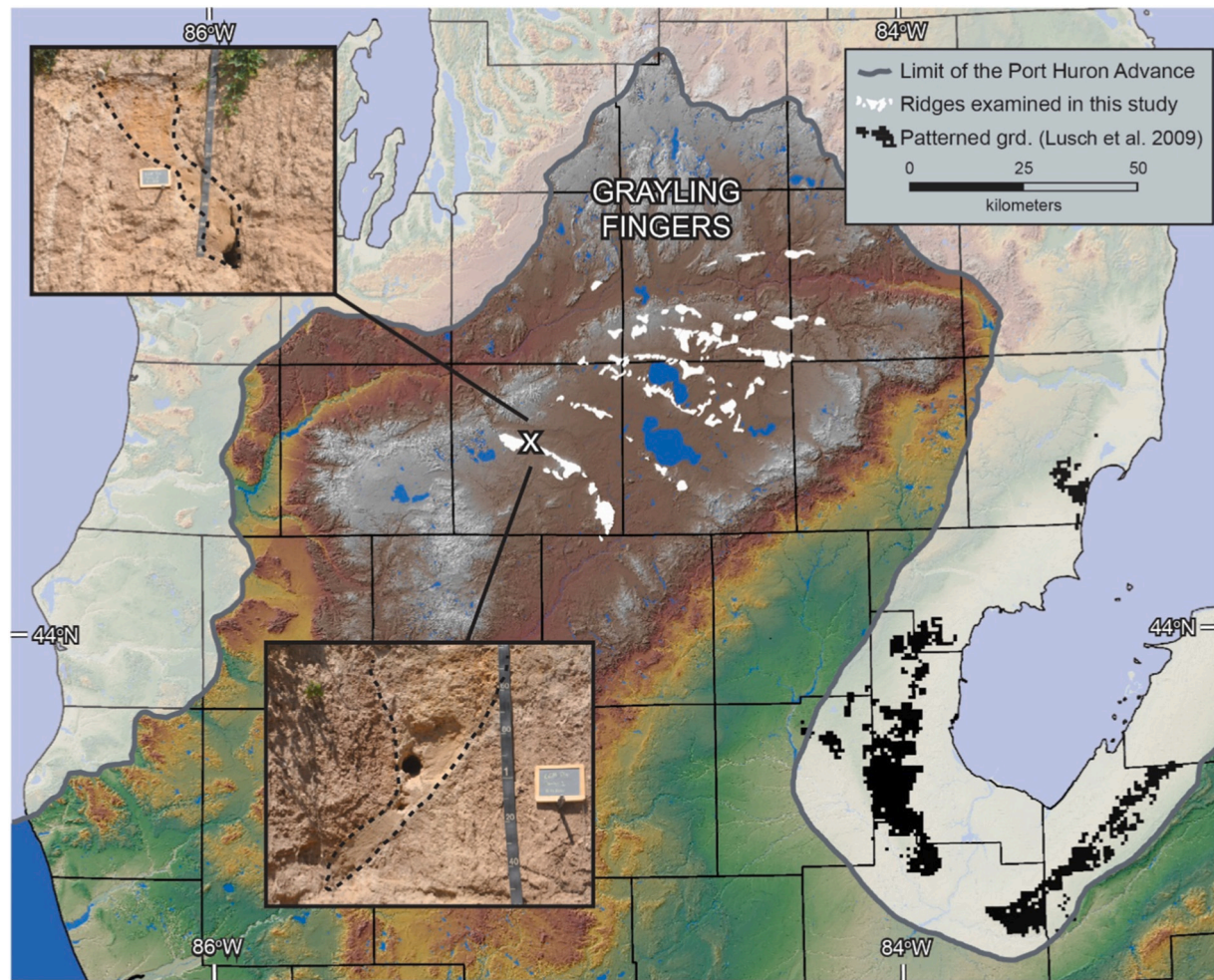


Fig. 4. Map of the ice margin position at the time of the Port Huron advance (ca. 15.2 ka). White polygons represent ridges, generally within the Houghton Lake Basin, i.e., the area under study here. Two images of well-formed ice wedge casts, commonly exposed in a pit in one of the more southern ridges, are shown. Areas with patterned ground are from Lusch et al. (2009).

easier, and avoid any significant losses in interpretability, we down-scaled these data into a digital elevation model (DEM) with a 2-m cell size. We then hand-placed a point at the lowest outlet position of each channel network to delineate its mouth/terminus (Fig. 5A). In total, 10,071 discrete gullied or other incised channel systems were identified.

Using the gully-mouth point data, we next delineated upslope contributing areas and channels, as well as downslope channels, for each gully-mouth point, using the Geographic Resources Analysis Support System (GRASS) GIS software package (GRASS Development Team, 2022; Fig. 5B). This hydrological mapping procedure began by first generating a single-flow (D8) direction, surface hydrology model at a 2-m scale resolution. This method iteratively identifies the cell within a 3×3 cell window (36 m^2) that has the lowest elevation, and then routes the surface flow and hydrological accumulation from all the (upstream) neighboring cells through that cell (O'Callaghan and Mark, 1984). The minimum flow accumulation for these channels was set to 199 cells, i.e., each pixel must have had a contributing area ≥ 199 cells (796 m^2) to be considered part of a channel. The output from this effort delineated small channels (strings of connected, high-accumulation pixels), usually along or near the centerlines (or thalweg) of the gullies and their associated drainage basins. Because our initial assessment of the gully-mouth locations did not always align exactly with these stream channels, we used the Snap tool in ArcMap to manually shift the gully-mouth points onto the nearest flowpath polyline, but staying as close as possible to what we perceived as the gully mouth. We then inspected the gully-

mouth point shapefile to ensure that all of the points aligned with a channel - an example of a student-led, Quality Control (QC) step.

Using the QC'd gully-mouth points, upstream drainage basins were then delineated in GRASS (GRASS Development Team, 2022); each basin included the land that contributed flow to that point (Fig. 5C). Subsequent spatial and topographic analyses only included pixels within the drainage basin upstream of the gully-mouth point. All future work was then based on basins, i.e., each basin was assigned a number in the GIS attribute table and subsequent data were added according to basin number.

The previously generated stream polylines (Fig. 5B) were intentionally drawn with small contributing areas, to visualize even the smallest potential fluvial channels. Fieldwork confirmed that most of these flowlines were far too small and subtle to be considered a "fluvial channel". Moreover, in larger channels, these flowlines often continued well beyond (above) the channel scarp (Fig. 5 A-B). Therefore, we modeled a second set of stream polylines, using a much larger contributing area (1000 cells, 4000 m^2) threshold (Fig. 5D). Although simplified, these stream polylines more accurately reflect natural channel networks across the study area, and were subsequently used to guide a drainage basin ordering procedure, i.e., each basin was assigned an order, from zero-order to third order (Warntz, 1975). Drainage basins assigned an order of zero were those that contained a single, visually discernible channel, but no flowline in the generalized polyline dataset. The basin ordering data were QC'd by having each student review the

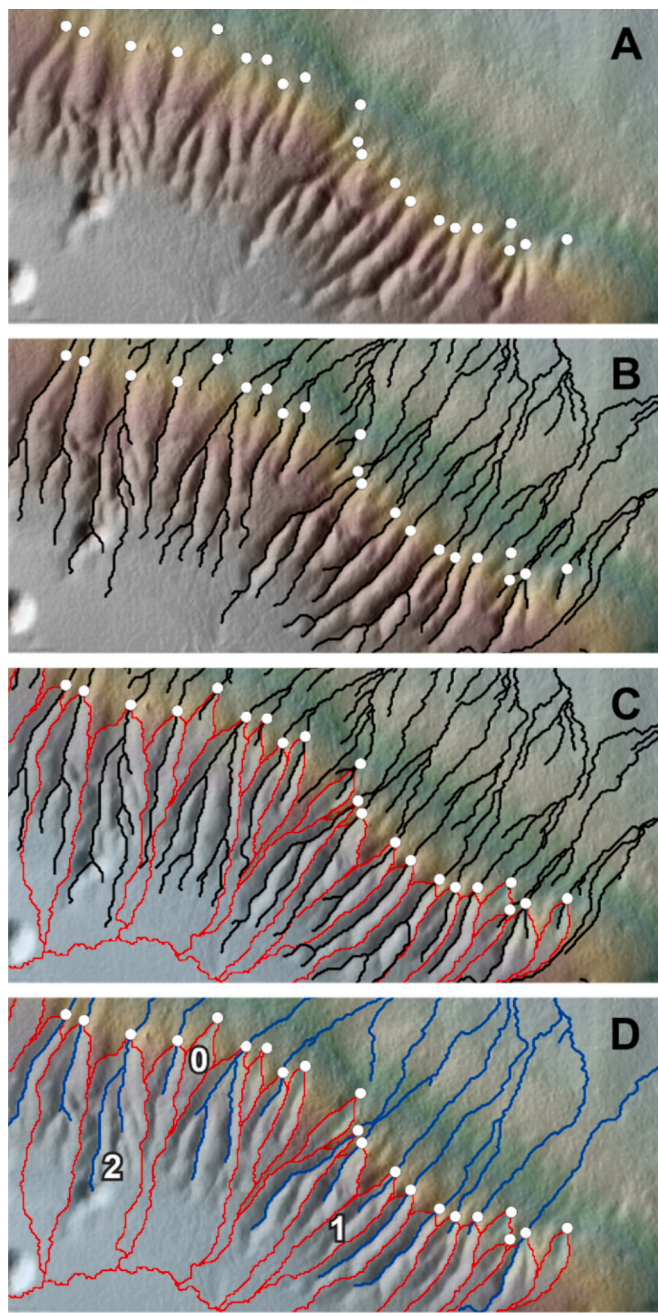


Fig. 5. Graphical illustration of the steps taken to delineate, map, and order the gully networks and basins. (A) Points (filled circles) marking the mouth/terminus of several gully networks, as identified through visual inspection of a 2-m LiDAR DEM. (B) Initial stream network model showing flowpath polylines routed along or near the thalweg of the gully channels. (C) Drainage basins delineated from the initial stream network model considering the contributing area upstream of each mouth/terminus point (5A). (D) Examples of 0th, 1st, and 2nd order basins based on a more simplified stream network model.

basin orders that had been initially assigned by a different student.

At this point, we initiated an additional QC procedure to identify and delete drainage basins that may have been affected by cultural features such as roads or gravel pits, or which (very few instances) had overlapping boundaries. Lastly, because we were planning to develop a variety of metrics for each basin, many of which would be based on topography, we also deleted or “clipped” some basins that contained a deep glacial kettle or several small ones, as these depressions would have impacted our data on basin depth and relief. We next preliminarily

examined a variety of topographic properties for the remaining 8880 basins and concluded that the 55 3rd order basins had very different attributes than the remainder of the (lower order) basins, and thus, were eliminated from subsequent analyses. Specifically, the 3rd order basins tended to have deeper channels, more integrated drainage networks, and indications of occasional influence of baseflow due to their overall lower position on the landscape. Thus, we anticipate that incision in these basins was influenced by different geomorphic conditions. Our final data set contained 8825 gullied basins.

3.2. Data compilation

3.2.1. Morphological and spatial characteristics

A variety of data were assembled and analyzed for each of the gullied basins. For each basin, we had already determined (manually) its order (0th, 1st, or 2nd). In ArcMap, we also determined basin area (m^2). A key metric that we next developed was basin depth – an indication of the depth of incision in each basin below a “pre-erosional” datum. To determine basin depth, we first created a DEM that mimicked the initial (pre-erosion) land surface. Because this land surface would not have been deeply incised with gullies, i.e., it would have been much “smoother”. We refer to this raster file as a “smooth DEM” (Fig. 6). We drove the creation of this DEM by generally aligning it with (spanning) the interfluves between the gullied basins. Creating the smooth DEM was accomplished in sequential steps. First, we extracted just the pixels from the original, 2-m DEM that fell along the basin boundaries (Fig. 5C) and converted them to points. We then interpolated these points with inverse distance weighting (power = 2, $n = 8$) to an 8-m raster across all the ridges/interfluves and resampled the raster to 2-m resolution with bicubic interpolation. Pixel-wise depths were then calculated by simple subtraction of the two rasters, i.e., smooth DEM values minus modern land surface values. Such values should be nearly zero for basin locations along the interfluves and above the channel scarp, but positive (in meters) above gully locations. Thus, for each basin, we developed a suite of depth metrics, reflective of the amount of postglacial incision by fluvial and slope processes. Because of statistical outliers in this large data set, we calculated not only mean values for these metrics, based also on data associated with the 75th and 90th percentiles of the depth (incision) data. Mean basin depths, for example, indicate the mean depth of the entire land surface in the basin, i.e., for all pixels, below the elevation of the smooth DEM. Maximum depth data were recovered from only the one “deepest” pixel in each basin.

Several additional metrics were then derived from the smooth DEM, as described below. The mean compass aspect of each basin was derived by calculating the circular mean of the aspects of all pixels in that basin. We also calculated metrics of slope gradient (mean, 75th, and 90th percentiles) for each basin by using a steepest downhill gradient algorithm (Jasiewicz and Mickiewicz, 2023) to calculate the slope gradient for each pixel, and then finding the mean, 75th, and 90th percentile values within each basin.

To test the hypothesis that permafrost was a factor in forming the gullies (Fig. 1), we examined in detail the compass aspect of the basins. At this latitude and on sloping surfaces, microclimates vary considerably across different aspects. We assumed that N and NE aspects at this latitude are comparably cooler and moister, with potentially more water available for surficial processes, e.g., Hunckler and Schaetzl (1997), Burnett et al. (2008), Donaldson et al. (2023), Saeidi et al. (2023). Conversely, S and SW aspects receive more insolation and thus may have had thicker active layers while permafrost was present. Thus, we focused our statistical analyses on the relationships among incision depths and slope gradients, as affected by aspect. Once determined, each of the aspect values was grouped into three categories: northeast (NE), southwest (SW), and cross slopes (cross) (Fig. 7). To test the differences between incision depths and slope gradients across the three aspect groups, we ran one-way ANOVAs. In instances where significant differences were found between the groups, we ran post-hoc Tukey's tests

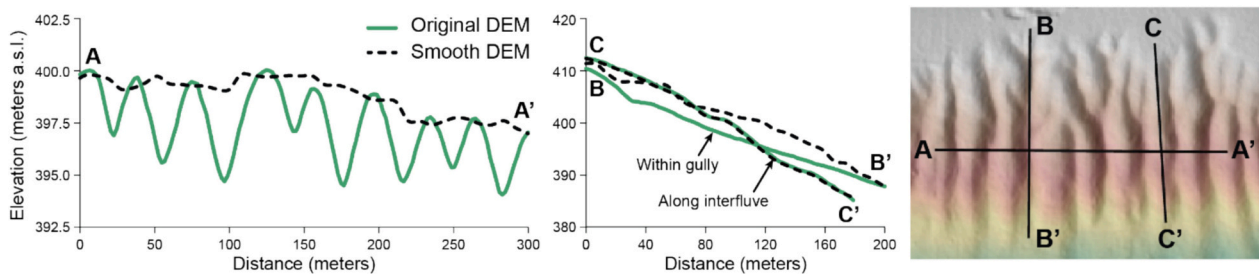


Fig. 6. Illustration of the smooth DEM vs the modern land surface, along three topographic transects. Note the excellent correspondence between the modern-day interfluve (assumedly a remnant of the pre-incision surface) and the smooth DEM.

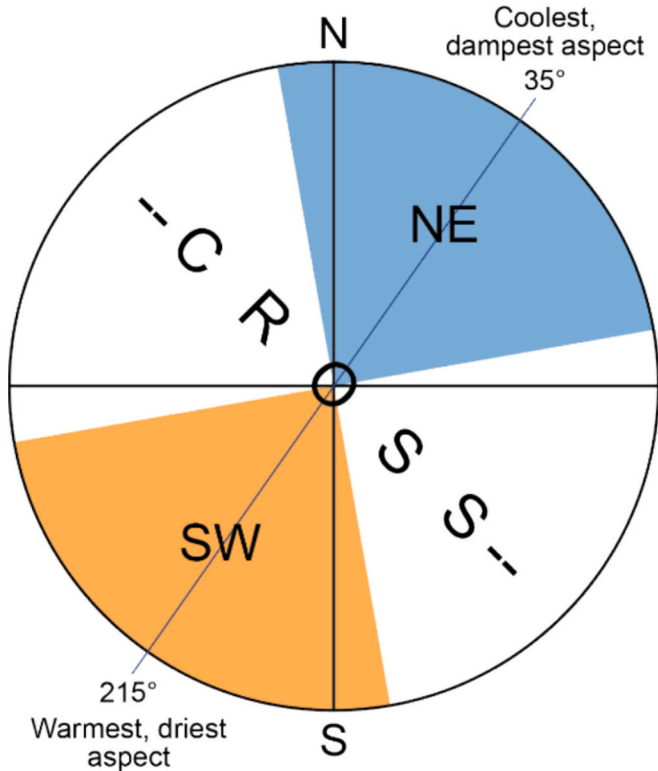


Fig. 7. Illustration of how we partitioned basin aspects into three categories, NE, SW and Cross, based on their assumed microclimates.

to analyze which groups were different from each other. We also ran a linear regression to test the relationship between incision depth and slope gradient, and an ordinary least squares regression (OLS) to see if the relationship differed by aspect group. These statistical tests assume a normal distribution, so the data distributions were assessed visually. Although the distributions of slope gradients was normal (with a slight right skewness), the incision depth data were not skewed. To fix the former, we used a log transformation, which made the incision depth variable have a normal distribution. OLS residuals were also assessed to confirm that errors were evenly distributed.

It should be noted that, with a dataset this large ($n = 8825$), even small differences will result in statistically significant p -values. Thus, the effect size (mean and slope estimates) and explained variance (R^2) are more meaningful for these tests than the p -values. All data analyses were performed in R (version 4.3.3), and for the OLS model comparison to the null model were done using AIC comparison with the *bbmle* package.

As has been done in other gully studies (Nicu et al., 2022), we also calculated a measure of convexity/concavity of the longitudinal profile of the channels in the gullies, using the initial channel data set (Fig. 5B). This work applied a channel concavity index (CI), first developed by

Langbein (1964) and applied recently by Phillips and Lutz (2008). The index determines the deviations in elevation from a straight-line profile, along a given channel. Rather than assess the longitudinal profile for every basin, we chose a subset of 381 first-order basins, each deemed “typical” of the surrounding basins. We chose to use only first-order basins, as they have one clearly defined channel. Zero-order basins have less well-defined channels and thus were not used in this analysis. Each of these basins already contained a gully-mouth point. We then added a point near the upper part of each basin and calculated, in GRASS, the route of water as it would have flowed down-basin, from this upper point to the gully mouth. The elevations of each 2-m pixel spacing along this route constituted the longitudinal profile for that basin, which were then used to calculate the CI. CI values range from -1.0 to $+1.0$, with a value of 0.0 indicating a perfectly linear longitudinal profile. Positive values indicate concavity; negative values indicate convexity.

Lastly, we examined incision depths along a longitudinal gradient across the study area, on the assumption that the more northerly ridges might have deeper gullies because of longer-lasting permafrost, i.e., they were farther up “in the refrigerator”. This was accomplished by assessing basin depth values (90th percentile) as a function of distance from a point in the far SW corner of the study area.

3.2.2. Sedimentology and soil development

To characterize the sediments in the study area, we sampled along four well-developed channel networks; each exhibited clear indications of some kind of fan at their mouth, enabling us to obtain data on the down-valley, sediment-receiving parts of the gullies as well as their channels. Samples of 400–500 g were taken at 40-m intervals along the gully thalweg and onto its fan. At each sample location, we collected the uppermost meter of soil by bucket auger, and homogenized the material in the field. In the lab, the samples were air-dried and passed through a 2-mm sieve to remove coarse fragments. Additional sieving enabled us to determine the 1–2 mm fraction (very coarse sand). The remaining fraction was pretreated by shaking for 15 min in a water-based solution of $(NaPO_3)_3 \cdot Na_2O$, followed by analysis on a Malvern Mastersizer 2000E laser particle size analyzer, for grain-size analysis.

We also examined the degree of soil development on a representative ridge in the study area, on the assumption that, if the gullies are, in fact, actively eroding, or even slightly unstable, the gully soils should be thinner and less developed than the soils on the interfluves, or even off the interfluves. We selected the ridge immediately south of Higgins Lake (Fig. 3) to minimize potential effects of site proximity to the ice margin (as described above). Across the ridge, we sampled gully-interfluve pairs at 20 sites and recorded data on A and E horizon thicknesses as indicators of the degree of soil development, given that podzolization is the dominant soil forming process in this region.

4. Results and discussion

4.1. Gully and basin morphometry

Each of the 72 ridge polygons in the study area (Fig. 3) contained at

least a few gullies/basins; many of them contained hundreds of gullies and incised channels. Where the slope of the upland was straight in plan view, many of the gullies occur in nearly idealistic, parallel drainage patterns, with few or no tributaries (Fig. 2).

The gullies appear topographically “sharper” and more incised (deeper) “on screen” (using LiDAR data; Fig. 2) than they do in the field (Fig. 8). In cross-section, the channels typically have relatively flat beds and smooth, rounded, upper margins; we have yet to find any evidence of an actively retreating upper slope within a larger alcove area, or an actively eroding headcut or scarp. All the gullies are dry channels with no evidence of any form of channelized runoff at present. In short, even within densely gullied slopes, the landscape appears to be stable.

Determining the morphology of the pre-incision landscape was central to our study. Our smooth DEM attempts to mimic such a landscape. The slopes on the uplands, as determined from the smooth DEM more broadly, and also as indicated by the interfluves between the gullies more locally (Fig. 6), were more gently sloping than one might initially assume, based on the seemingly widespread occurrence of incision on the landscape (Fig. 2). Across all 8825 basins, including all of

the land surface, i.e., pixels, within them, the mean slope gradient was only 10.2 % (5.8°) (Table 1). Omitting the steepest sections of each basin, i.e., calculating the 90th percentile of basin slope gradient, still yields a mean basin slope of only 16.1 % (9.1°) (Table 1). These values

Table 1
Descriptive metrics for the gullies and their basins (complete data set).

Metric	Mean value	Median value	90th percentile value
Basin area (m ²)	11,684	7368	26,347
Basin slope gradient (from smooth DEM; including all pixels in the basin) (%, °)	10.2; 5.8	9.3; 5.3	16.1; 9.1
Basin incision (maximum depth of incision, based on data from the “deepest” pixel in the basin [smooth DEM minus modern land surface]) (m)	2.8	2.0	5.7

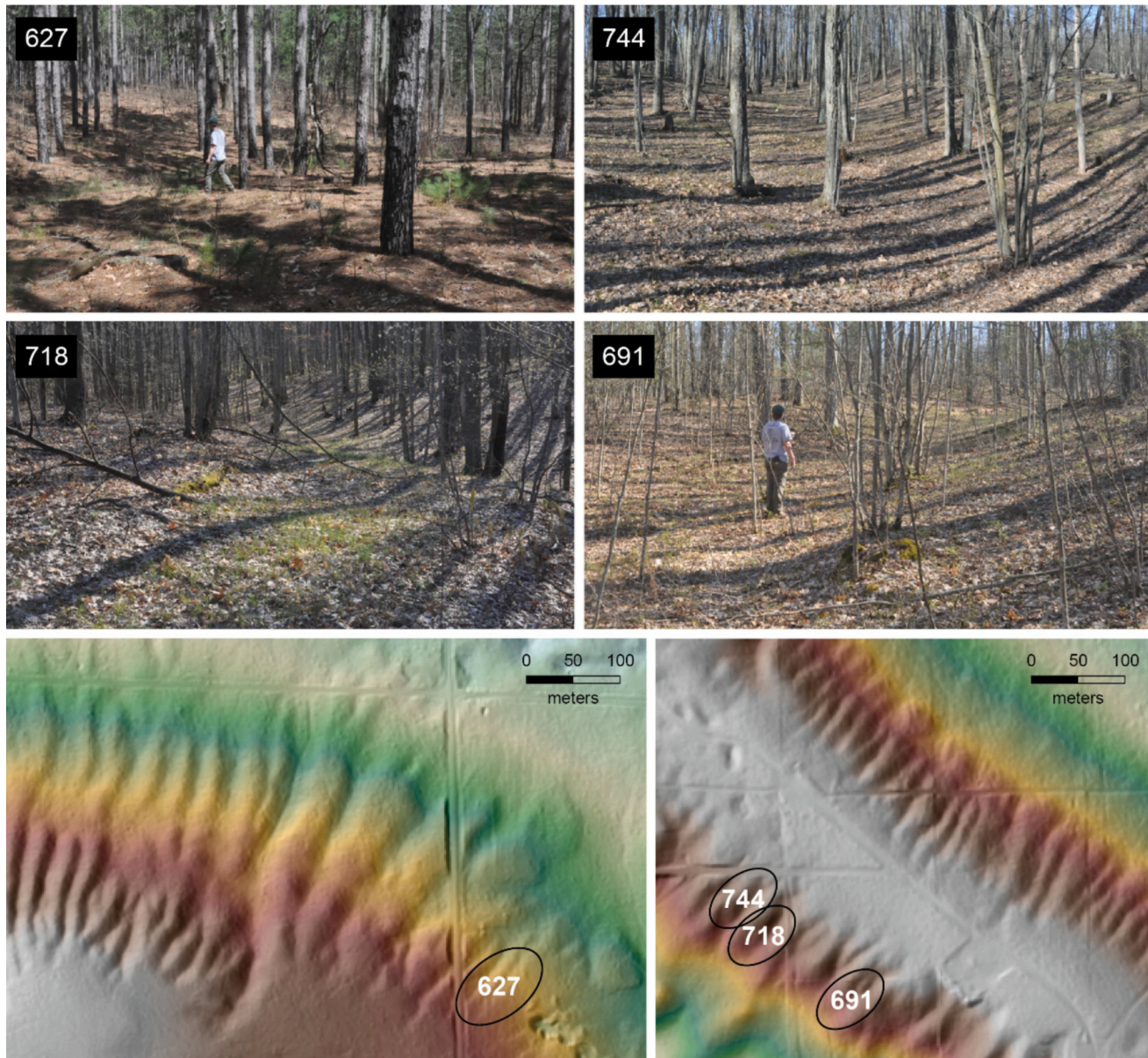


Fig. 8. Photos of gullies in the field, vs their appearance in a hillshaded GIS image. Numbers shown derive from our basin-numbering data set. Photos by RJS.

are well below the repose angle for sand ($15\text{--}45^\circ$), as well as critical slope values typically reported for hillslopes that have (or are experiencing) gullying (Vandaele et al., 1996). It is difficult to imagine any kind of precipitation or snowmelt event that could currently generate enough runoff in these sandy basins, especially on such fairly gentle slopes.

ANOVA data, as well as post-hoc Tukey's tests, confirmed that basin slope gradients were significantly different among the three aspect groups ($p < 0.001$; Fig. 9). Slope gradients were generally steepest in the NE basins, largely because many of these basins would have formed on former ice-contact slopes (Schaetzl et al., 2017). SW-oriented basins were the most gently sloping of the three groups, again largely due to glacial history; many of these basins occur on slopes that would have been within depositional settings, such as outwash fans or deltas.

Our data for the 8825 gullies indicate that they are quite shallowly incised into the neighboring uplands (Fig. 10). Across the full data set, basins had an average maximum depth of incision, i.e., the difference in elevation of the deepest pixel in the basin below the smooth DEM, of only 2.8 m; the median value is 2.02 m (Table 1; Fig. 10). The distribution of incision depths is highly skewed, with a few basins having deep gullies, even as most of the basins have much smaller (< 4 m) incision depths (Fig. 10). Fig. 11 shows the median and various interquartile values of this same metric (maximum incision), broken out among the various aspect groups. Incision depths increase with increasing slope gradient (Fig. 12).

ANOVA data indicate, and post-hoc Tukey's tests confirm, that basin incision depths are significantly different among the aspect groups ($p < 0.001$; Fig. 11). Mean incision depths are actually similar between the NE and SW groups ($p = 0.87$) but different from the cross group ($p < 0.001$), which had the greatest incision depths (Fig. 11). It should be noted that the actual differences between the aspect groups in both slope gradient and incision depths are small, as is the amount of explained variance ($R^2 = 0.008$ for incision depth and 0.04 for slope gradient). Thus, aspect is not a strong explanatory variable for gully formation/incision, as gullies have formed almost equally well on slopes of all aspects (Figs. 12, 13). The deepest incision values occur in NE-facing basins, probably because these aspects are more often steeper (Fig. 9). In conclusion, we observe that (1) the amount of incision in most of these basins is typically only about two meters deep (Table 1; Fig. 10), and (2) aspect alone does not appear to be a strong explanatory variable for incision on this landscape (Figs. 12, 13).

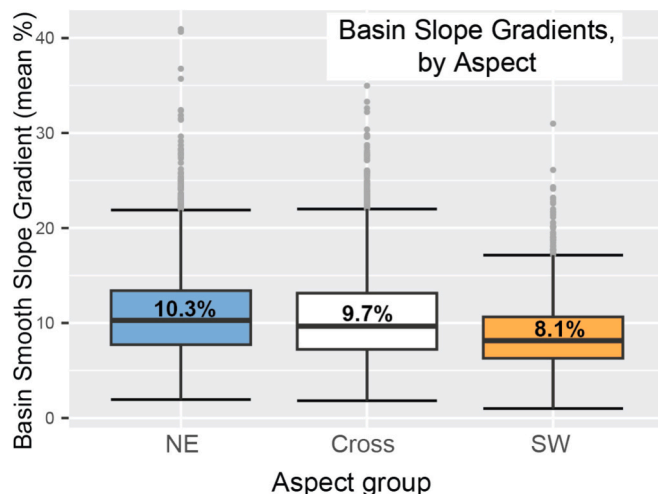


Fig. 9. Slope gradients, as determined off the smooth DEM and classified by aspect (see Fig. 7). The centerline of each box is the median value, the box itself represents the interquartile range or IQR (25th to 75th percentiles), the whiskers are ± 1.5 times the IQR values, and the dots are data points beyond the whisker threshold.

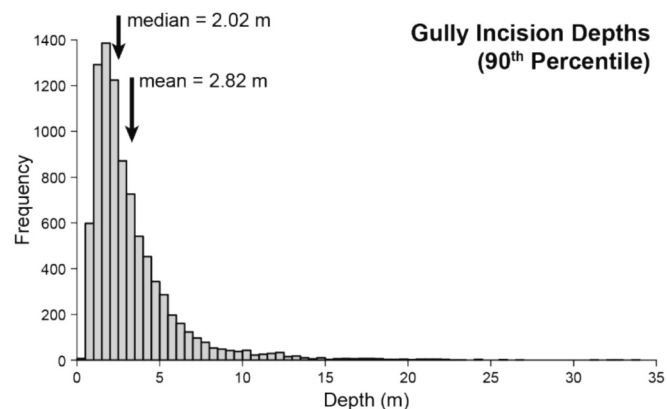


Fig. 10. Histogram showing the distribution of maximum incision depths (90th percentile) in all 8825 basins, including central tendencies.

We suggest that the influence of aspect on gully development may actually be masked by differences in slope gradient. Under a periglacial regime, increased insolation on S and SW facing slopes should have resulted in greater active layer thicknesses, more available water, and thus, more erodible substrates. Other things being equal, it would therefore be expected that gullying processes, if indeed controlled by permafrost and active layer dynamics, should have been enhanced on the S and SW facing slopes. However, because these slopes have an overall shallower gradient, a thicker active layer would have likely been required to allow for an equivalent degree of incision to occur. Therefore, on the N and NE facing slopes, despite a thinner seasonal active layer, incision could ultimately keep pace due to the higher potential energy resulting from the steeper gradient. This effect may have been further facilitated by the presence of a more persistent permafrost table on the N and NE facing slopes, allowing erosion and incision to proceed for a longer period of time. In short, slope gradient effects may have "cancelled out" the microclimatic effects of aspect.

In addition to being only weakly incised into the sandy sediments in the ridges, the gullies in the study area are also distinctly parallel and often unbranched in plan view, and linear in their longitudinal profiles (Fig. 14). The median gully has a minimally concave longitudinal profile, suggestive of an ephemeral channel that may have flowed very infrequently and with low stream power. Some channels are even convex in longitudinal profile (Fig. 14C). Phillips and Lutz (2008) concluded that convexities in longitudinal profiles are generally caused by inherited topography, geologic controls, recent and contemporary geomorphic processes, and anthropogenic effects (cf. Bowman et al., 2007). On the slopes of the study area, where sediments are uniformly sandy, downstream changes in geologic/lithologic controls are minimal. Likewise, anthropogenic effects are negligible. And because the gullies are currently stable, "contemporary geomorphic processes" have had little effect on their formation. Rather, the channels generally follow the gradient of the surrounding slope, with only minimal amounts of incision. Thus, the longitudinal profiles of the gullies generally reflect the original shape of the sideslopes on which they have formed, i.e., the inherited topography. Indeed, Phillips and Lutz (2008) argued that convex or low-concavity profiles more often reflect local environmental constraints and geomorphic histories than any kind of local "disequilibrium".

Assessment of basin depth values (90th percentile) as a function of latitude (i.e., proximity to the ice margin) yielded little or no correlation between gully depths and location (Fig. 15). We interpret these data to mean that the entire study area was equally rife with permafrost.

4.2. Gully and fan sedimentology

Across the study area, fans and depositional landforms that one

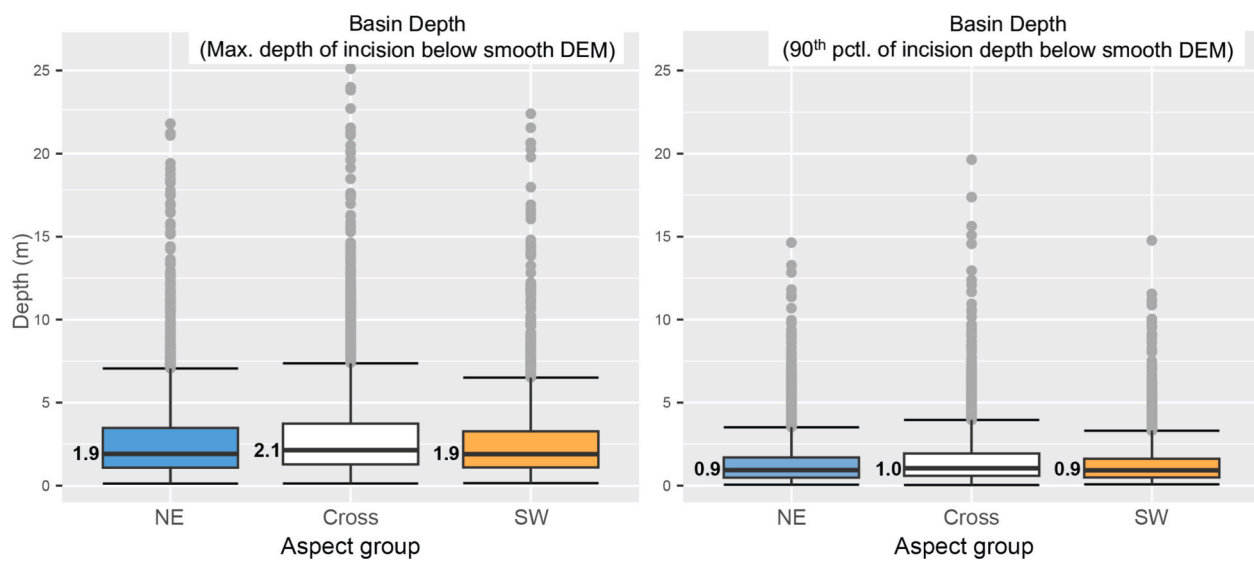


Fig. 11. Two different measures of maximum basin incision, i.e., gully depths, as classified by aspect (see Fig. 7). Symbology is similar to Fig. 9.

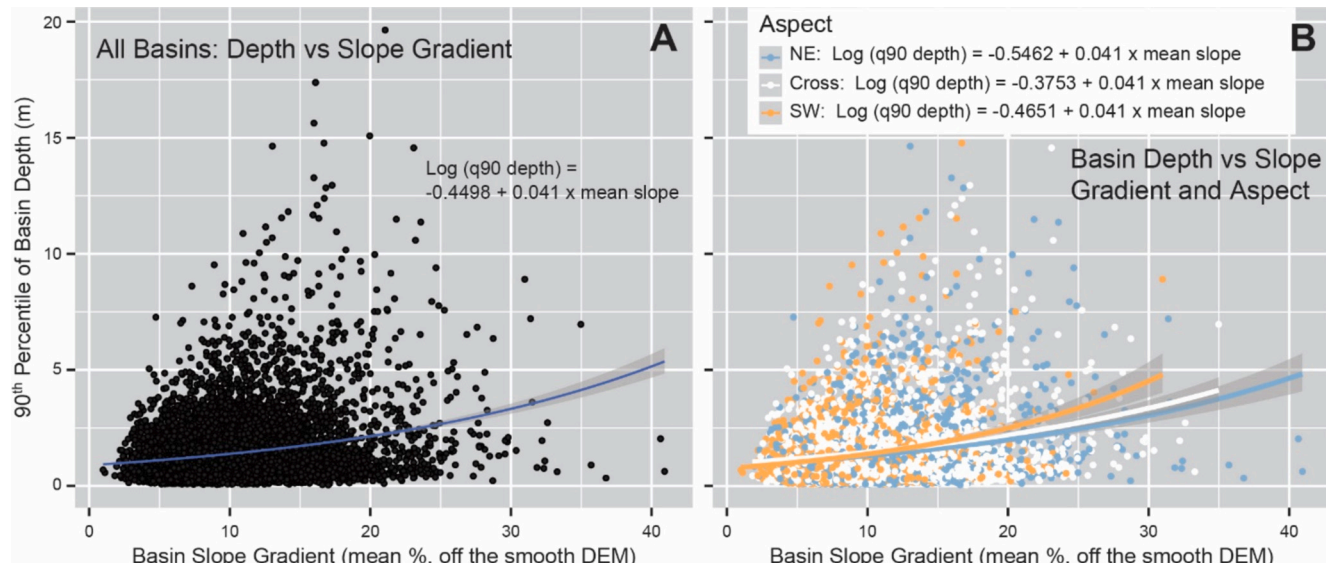


Fig. 12. Amount of basin incision (90th percentile of incision depth, below the smooth DEM), as a function of mean slope of the basin (also from the smooth DEM). A. All basins. B. Basins split out by aspect (see Fig. 7).

would expect to exist at the mouths of gullies and channels are often absent, and where present, only minimally developed. We take this as evidence of minimal sediment transport within these small, shallow channels, as supported by gully depth data (Figs. 10, 11). In many instances, the lack of clear, fan-like features at most gully mouths can be explained by coalescence, i.e., a broad, gently sloping apron of accumulated material has formed along the ridge footslope, rather than as discrete fans. It is also possible that sediment delivered to the gully mouths was dispersed so widely, because of underlying, ice-rich permafrost, that fan-like landforms did not form (Fig. 2).

As mentioned above, we sampled sediments down the axis of four gully systems and later classified the samples according to location – gully/channel, transitional, and fan. These sites were chosen because they did have small fans at the gully mouth location.

Grain-size data for the 20 samples from the channels in the four gullies indicate their coarse, sandy textures; the sediments averaged $86.9 \pm 3.8\%$ sand, $8.8 \pm 2.7\%$ silt, and $4.3 \pm 1.3\%$ clay (loamy coarse sand texture). Medium ($35.8 \pm 5.5\%$) and coarse ($28.9 \pm 9.1\%$) sands

dominated. Each of the four sampled gullies had a small depositional feature, or fan, at its distal end. The 16 samples taken from these fans are very similar to, if not even slightly coarser than, the sediments in the gully channels: $87.4 \pm 5.1\%$ sand, $8.6 \pm 3.3\%$ silt, and $4.0 \pm 1.9\%$ clay (loamy sand). Mean-weighted grain size data indicate that sediments actually become coarser down-fan (Fig. 16). Together, these data indicate that the landforms are very coarse-textured overall and that down-valley sediment sorting processes were only minimally active. The lack of sorting across the fans (Fig. 16) may even suggest the influence of slope processes, such as solifluction, within parts of some of the gully systems.

4.3. Gully soils

Schaetzl's (2008) data from the Grayling Fingers (Fig. 4) indicated that gullies in this region are, at present, geomorphically stable. This conclusion was based on metrics designed to indicate the degree of soil development within the various microtopographic positions on the

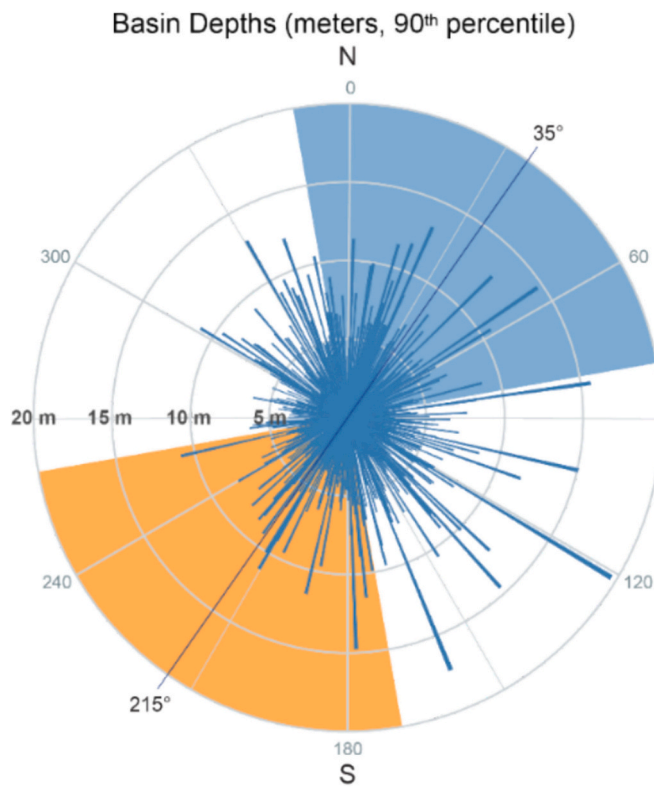


Fig. 13. Compass rose showing 90th percentile of incision depths (smooth DEM minus modern land surface), plotted by basin aspect, for all 8825 basins.

landscape. In short, soil development in the Grayling Fingers' gullies is as strong or stronger than on nearby interfluviums, and also stronger than on nearby stable, flat surfaces.

As observed in the Grayling Fingers regions, soil development within the gullies in our study area, as indicated by soil horizon thicknesses, is

similar to, or thicker, than on the nearby interfluviums (Fig. 17). Gully E horizons are actually >4 times thicker than on interfluviums, probably due to the increased percolation (not less, as would be expected if they were runoff sites) they receive from spring snowmelt; snow drifts into the gullies and drifts off the interfluviums. If the gullies were actively eroding, or even slightly unstable, the soils would be thinner and less developed than on the adjacent interfluviums. These data, along with many instances of field study, during which we never observed any evidence of active erosion or runoff within gullies, confirm that the gullies in the study area are currently stable. Thus, we conclude, as did Schaetzl (2008), that the gullies are relict features from a former interval of geomorphic instability.

4.4. Genetic interpretations

As indicated by a variety of data, gullies in our study area show only minimal fluvial incision (Figs. 10, 11) and poor downstream sorting (Fig. 14). Even on steeper slopes, incision depths varied little (Fig. 12A), and most channels have nearly linear longitudinal profiles that closely mimic the underlying slope (Fig. 14). Together, these data point to incipient, ephemeral fluvial systems that eroded small channels into these sandy slopes (Figs. 5, 8). Despite the constraints on these systems, erosional processes were able to incise into almost every ridge in the study area, and into many more outside the study area. This impressive amount of erosion - across such a large area and on sandy, moderate slopes - must have been assisted by permafrost, in order to facilitate runoff on an otherwise highly permeable substrate. Indeed, the strong soil development within the sampled gullies suggests that they have been stable for an extensive period of time, perhaps since the Late Pleistocene. Given these considerations, we suggest that gully formation across the study area - widespread in scope but with only minimal amounts of incision - was driven by thermo-erosion processes, i.e., the seasonal thawing of ground ice (Kokelj and Jorgenson, 2013), on a former periglacial landscape. Thus, the gullies in the study area might be more correctly termed thaw gullies or thermo-erosion gullies (Kokelj and Jorgenson, 2013).

In a thermo-erosion model, sediment below the active layer remains

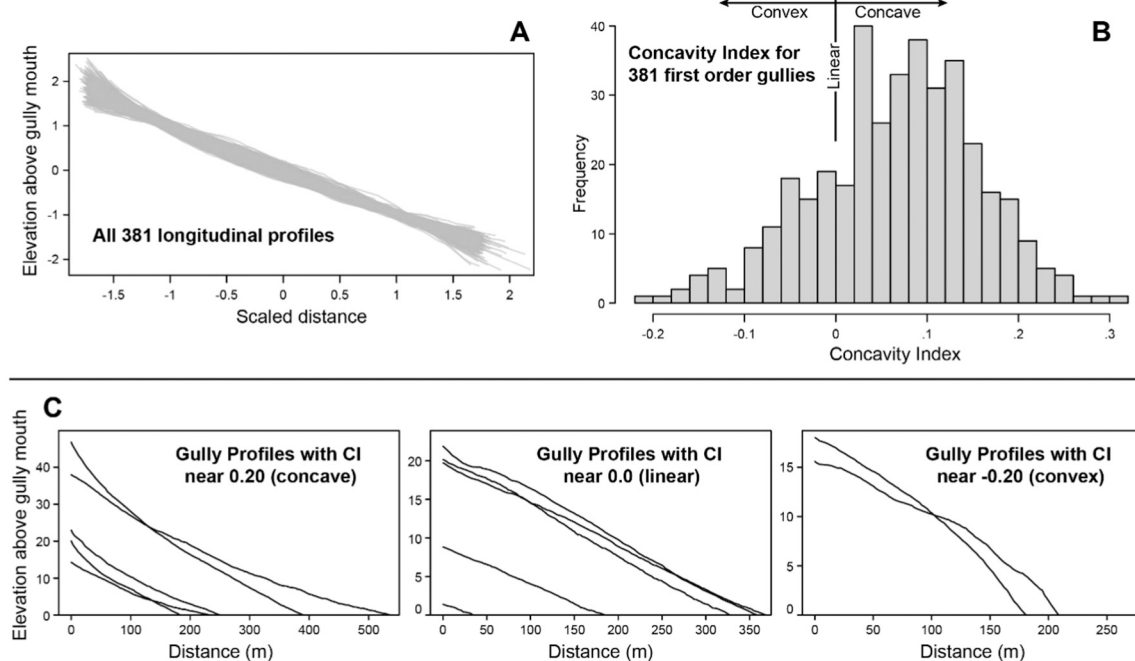


Fig. 14. Longitudinal profiles of typical gullies in the study area. (A) A compilation of the longitudinal profiles of all 381 gullies, each scaled to approximately the same horizontal distance. (B) Histogram of channel concavity index (CI) values for the gullies, compiled at intervals of 0.05. (C) Typical profiles for some gullies that have concave, linear, and convex longitudinal profiles.

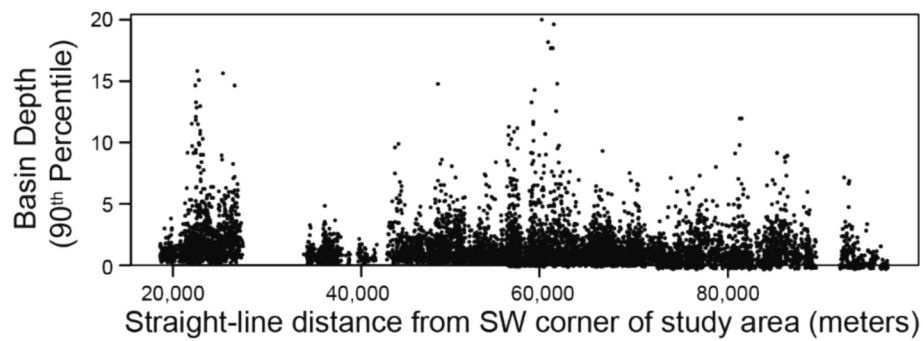


Fig. 15. Gully depths (90th percentile) in basins, as a function of distance from a point in the far SW corner of the study area.

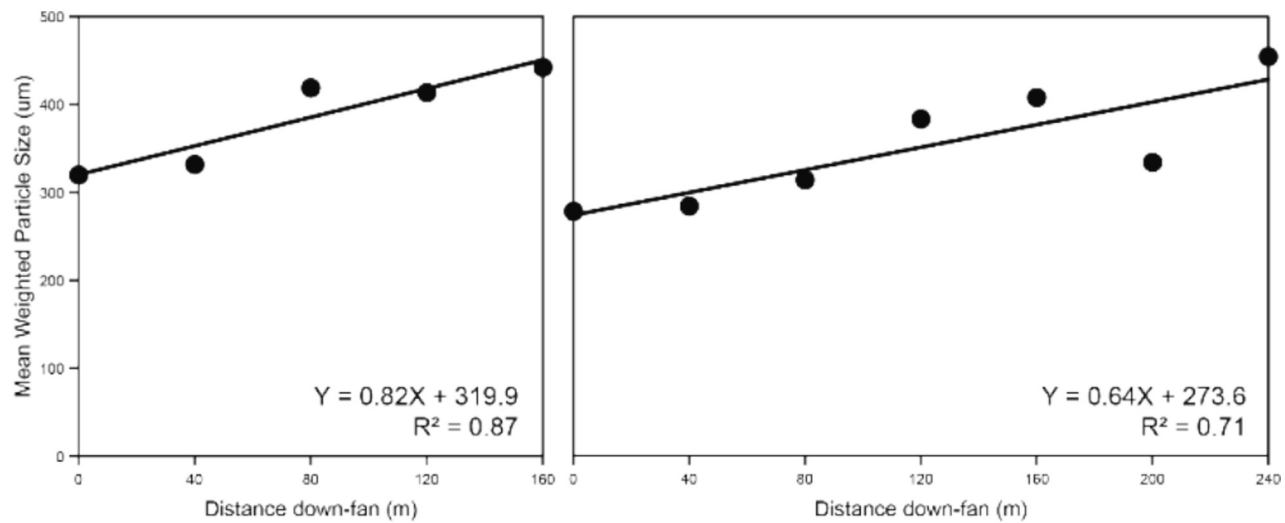


Fig. 16. Mean weighted particle size data for two fans at the distal ends of gullies. Although we sampled the soils along four gullies and their corresponding fans, the other two fans were so small/short that they had fewer than five samples, and thus, are not shown here.

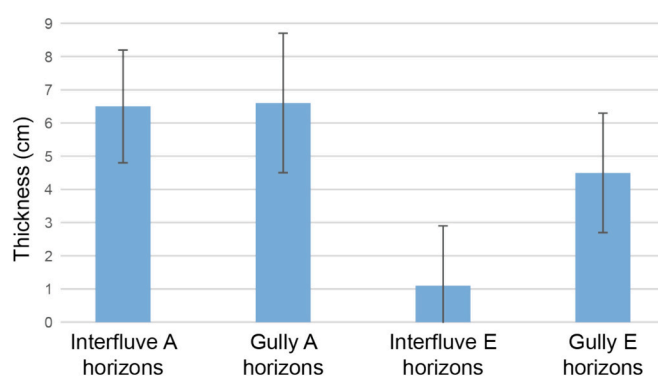


Fig. 17. Mean horizon thicknesses (and standard deviations) for soils in a representative gully and its neighboring interfluvia.

permanently frozen, often with ice contents exceeding 75–90 % in its upper part (Iwahana et al., 2014). As it thaws, this ice-rich layer releases water to the active layer above. Areas of surface water convergence within the active layer, known as water tracks, become saturated. Water tracks may concentrate water within both aboveground and subsurface flow pathways (Trochim et al., 2016; Paquette et al., 2018; Del Vecchio et al., 2023). Increased pore water pressures at the base of the active layer may also initiate thaw slumps and other types of shallow mass flows (Mann et al., 2010; Nicu et al., 2022); these types of slope processes may explain some of the inverse down-fan sorting we observed

(Fig. 16). Surface runoff may generate small scale fluvial erosion and, thus, form incipient channels. Fluvial channels may form and enlarge over time, assisted by advective heat transfer in the running water (from the water to the permafrost). These processes may promote positive feedbacks, i.e., as channels deepen they collect more snow in winter and transport more runoff in summer, enhancing thermo-erosion and further deepening the channel (Godin and Fortier, 2012; Nicu et al., 2022). As surface water becomes increasingly channelized on ice-rich substrates, gullies may continue to deepen, as particles destabilize and sediment transport becomes more pronounced (Jorgenson and Osterkamp, 2005). This interplay of surficial (geomorphic and hydrological) processes may be geomorphically weak to begin with, but as soon as channels are formed and/or the climate warms, feedbacks may strengthen the process. Thus, thaw gullies grow upslope by headward erosion and by deepening and widening of the channel. Eventually, with the complete thawing of the permafrost, runoff becomes minimal and erosion processes slow and stop. The land surface stabilizes, and soils formation begins to outpace other surficial processes.

On sloping surfaces in midlatitude locations, aspect should have an influence on thermo-erosion processes (Imhof, 1996; Ma et al., 2015; Zwieback, 2021). For example, Mann et al. (2010) provided an excellent example of slides on a modern-day (thawing) tundra landscape, where most of the slope failures occur on south-facing slopes. In our study area, active layer thicknesses would have been thinner and permafrost and snowpacks should have persisted longer on cooler, NE slopes. Our data, however, show very little difference in incision depths on various aspects (Fig. 10). Again, this may point to slope gradient as a more dominant control on hillslope processes. Our analysis also indicated

little or no correlation between gully depths and location (Fig. 15), despite our assumption that the more northerly ridges might have experienced a greater degree of erosion because of longer-lasting permafrost, i.e., they were farther up “in the refrigerator”. We attribute this lack of correspondence to the fact that the gullies are usually <2 m deep, i.e., they are only weakly formed (Figs. 11, 12). If incision depths in these small gullies do differ as a function of location, these differences are too subtle to have been captured by our analyses.

Reasons for the minimal amounts of incision and lack of influence of slope aspect and latitudinal position under a thermo-erosional regime, as observed in our study area, can be ascribed to any or all of the following scenarios.

1. The permafrost interval did not last very long, but as indicated in Fig. 4 and as supported by data shown in Fig. 15, likely still covered the entire study area.

2. The climate was so cold and the permafrost interval so intense, with only minimal snowmelt and very thin active layers, that limited opportunities for runoff developed (McNamara et al., 1999). In this scenario, runoff could do little to incise into the frozen sediment.

3. Permafrost in these permeable, sandy soils did not develop large amounts of ice and thus, remained somewhat permeable, limiting runoff.

4. The paleoclimate was so dry, with only small amounts of water released from melting snow and/or falling as rain, that little water was available for sediment transport.

Schaetzl (2008) invoked permafrost to explain the formation of gullies in the nearby Grayling Fingers region, which facilitated runoff and erosion. This mechanism has also been proposed to explain the occurrence of relict gullies with similar morphometry, i.e., shallow depths, flat channel beds, and smooth, rounded upper slope margins, in coarse-textured sediments in other former near-ice marginal settings (Langohr and Sanders, 1985; Panin et al., 2009; Soms, 2011). Using such a model, the gullies in our study area must have formed in the immediate postglacial period, around the time of the Port Huron advance of ca. 15.2 ka, when the area was located in a major glacial reentrant (Fig. 4).

5. Conclusions

Our study reexamined the conclusions of Schaetzl's (2008) work in northern Lower Michigan as a testable hypothesis by obtaining data on thousands of sandy-but-gullied drainage basins and for each, determining their compass aspect, and estimating the amount of incision that each had incurred. Our findings suggest that permafrost was likely to have formed on this landscape in the early postglacial period and thus would have played a factor in gully incision by producing an impermeable or slowly-permeable layer at depth. The absence of runoff from the modern landscape, as indicated by well-developed soils in the gullies, necessitates this assumption. Sediments here average almost 90 % sand and <5 % clay.

Our study is the exception to most other reports of modern thermo-erosion gullies, e.g., Tsuyuzaki et al., 2001, in that the gullies have formed on coarse-textured substrates. Gullies in this study are also very different from thermo-erosion gullies elsewhere, in that they did not develop along polygonal networks or within a landscape with patterned ground (Paquette et al., 2018). There is no evidence of patterned ground on the sandy slopes of our study area, and neither would one expect there to be. Thus, our work provides a unique example of gully formation on a paleo-periglacial landscape, which may be useful to others who are studying the rapid changes to the hydrology of the contemporary Arctic and Antarctic, e.g., Levy (2015), Paquette et al. (2017), Rushlow and Godsey (2017), Biskaborn et al. (2019), Rushlow et al. (2020), Nicu et al. (2022).

CRediT authorship contribution statement

Christopher J. Baish: Writing – review & editing, Writing – original

draft, Methodology, Investigation, Conceptualization. Alanna Post: Writing – original draft, Methodology, Investigation, Conceptualization. Ashton M. Shortridge: Supervision, Methodology, Investigation. Randall J. Schaetzl: Writing – review & editing, Writing – original draft, Methodology, Investigation, Conceptualization. Parker Hopkins: Methodology. Anthony Bowman: Methodology. Isabella Rabac: Methodology. Bernard Frantz: Methodology. Andrew O. Finley: Software, Methodology.

Declaration of competing interest

I have nothing to declare.

Acknowledgements

We thank Jonathan Phillips for reviewing an earlier draft of this paper, and students and faculty in the Department of Geography, Environment, and Spatial Sciences for feedback and input on this project. Dave Lusch and Fritz Nelson provided important feedback at an early stage of the project. The research was supported by a grant from the National Science Foundation, Geography and Spatial Sciences Program (award #1759528).

Data availability

Data will be made available on request.

References

Attig, J.W., Hanson, P.R., Rawling III, J.E., Young, A.R., Carson, E.C., 2011. Optical ages indicate the southwestern margin of the Green Bay Lobe in Wisconsin, USA, was at its maximum extent until about 18,500 years ago. *Geomorphology* 130, 384–390.

Avni, Y., 2005. Gully incision as a key factor in desertification in an arid environment, the Negev highlands, Israel. *Catena* 63, 185–220.

Batchelor, C.J., Orland, J.J., Marcott, S.A., Slaughter, R., Edwards, R.L., Zhang, P., Li, X., Cheng, H., 2019. Distinct permafrost conditions across the last two glacial periods in midlatitude North America. *Geophys. Res. Letts.* 46, 13318–13326.

Belayneh, L., Kervyn, K., Gulie, G., Poesen, J., Stal, C., Kasaya, A., Endale, T., Sekajugo, J., Dewitte, O., 2024. Life cycle of gullies: a susceptibility assessment in the Southern Main Ethiopian Rift. *Nat. Hazards* 120, 3067–3104.

Biskaborn, B.K., Smith, S.L., Noetzli, J., Matthes, H., Vieira, G., Streletskiy, D.A., Schoeneich, P., Romanovsky, V.E., Lewkowicz, A.G., Abramov, A., Allard, M., Boike, J., Cable, W.L., Christiansen, H.H., Delaloye, R., Diekmann, B., Drodov, D., Etzelmüller, B., Grossé, G., Guglielmin, M., Ingeman-Nielsen, T., Isaksen, K., Ishikawa, M., Johannsson, M., Johannsson, H., Joo, A., Kaverin, D., Kholodov, A., Konstantinov, P., Kroger, T., Lambiel, C., Lanckman, J.-P., Luo, D., Malkova, G., Meiklejohn, I., Moskalenko, N., Oliva, M., Phillips, M., Ramos, M., Sannel, A.B.K., Sergeev, D., Seybold, C., Skryabin, P., Vasilev, A., Wu, Q., Yoshikawa, K., Zheleznyak, M., Lantuit, H., 2019. Permafrost is warming at a global scale. *Nat. Commun.* 10. <https://doi.org/10.1038/s41467-018-08240-4>.

Blewett, W.L., Winters, H.A., Rieck, R.L., 1993. New age control on the Port Huron moraine in northern Michigan. *Phys. Geog.* 14, 131–138.

Bogaart, P.W., Tucker, G.E., de Vries, J.J., 2003. Channel network morphology and sediment dynamics under alternating periglacial and temperate regimes: a numerical simulation study. *Geomorphology* 54, 257–277.

Bowman, D., Shachnovich-Firtel, Y., Devora, S., 2007. Stream channel convexity induced by continuous base level lowering, the Dead Sea, Israel. *Geomorphology* 92, 60–75.

Brown, R.D., Mote, P.W., 2009. The response of Northern Hemisphere snow cover to a changing climate. *J. Climate* 22, 2124–2145.

Burgis, W.A., 1977. Late-Wisconsinan History of Northeastern Lower Michigan. PhD Diss., Univ. of Michigan. 396 pp.

Burnett, B.N., Meyer, G.A., McFadden, L.D., 2008. Aspect-related microclimatic influences on slope forms and processes, northeastern Arizona. *J. Geophys. Res.* 113. <https://doi.org/10.1029/2007JF000789>.

Carson, E.C., Hanson, P.R., Attig, J.W., Young, A.R., 2012. Numeric control on the late-glacial chronology of the southern Laurentide Ice Sheet derived from ice-proximal lacustrine deposits. *Quatern. Res.* 78, 583–589.

Carson, E.C., Attig, J.W., Rawling III, J.E., 2019. The glacial record in regions surrounding the Driftless Area. In: Carson, E.C., Rawling, J.E. III, Daniels, J.M., and J.W. Attig. (eds). *The Physical Geology and Geography of the Driftless Area: The Career and Contributions of James C. Knox*. Geol. Soc. Am. Spec. Paper 543, 37–50.

Castillo, C., Gómez, J.A., 2016. A century of gully erosion research: Urgency, complexity and study approaches. *Earth-Science Revs.* 160, 300–319.

Clayton, L., Attig, J.W., Mickelson, D.M., 2001. Effects of late Pleistocene permafrost on the landscape of Wisconsin, USA. *Boreas* 30 (173), 188.

Conway, S.J., Balme, M.R., Kreslavsky, M.A., Murray, J.B., Towner, M.C., 2015. The comparison of topographic long profiles of gullies on Earth to gullies on Mars: a signal of water on Mars. *Icarus* 253, 189–204.

Conway, S.J., Butcher, F.E.G., de Haas, T., Dejins, A.A.J., Grindrod, P.M., Davis, J.M., 2018. Glacial and gully erosion on Mars: a terrestrial perspective. *Geomorphology* 318, 26–57.

Costanzo, S., Zerbini, A., Manzo, A., 2022. Active surface processes at Mahal Teglinos (Kassala, Eastern Sudan): Archaeological implications for an endangered protohistoric site in Sahelian Africa. *J. Archaeological Science-Reports* 43. <https://doi.org/10.1016/j.jasrep.2022.103452>.

Dalton, A.S., Stokes, C.R., Batchelor, C.L., 2022. Evolution of the Laurentide and Innuittian ice sheets prior to the last Glacial Maximum (115 ka to 25 ka). *Earth-Sci. Revs.* 224. <https://doi.org/10.1016/j.earscirev.2021.103875>.

Del Vecchio, J., Zwieback, S., Rowland, J.C., DiBiase, R.A., Palucis, M.C., 2023. Hillslope-channel transitions and the role of water tracks in a changing permafrost landscape. *J. Geophys. Res. Earth Surf.* 128, e2023JF007156.

Del Vecchio, J., Palucis, M.C., Meyer, C.R., 2024. Permafrost extent sets drainage density in the Arctic. *PNAS* 121. <https://doi.org/10.1073/pnas.2307072120>.

Dickson, J.L., Head, J.W., Levy, J.S., Morgan, G.A., Marchant, D.R., 2019. Gully formation in the McMurdo Dry Valleys, Antarctica: multiple sources of water, temporal sequence and relative importance in gully erosion and deposition processes. *Geol. Soc. Lond. Spec. Publ.* 467 (1), 289–314.

Donaldson, A.M., Zimmer, M., Huang, M.H., Johnson, K.N., Hudson-Rasmussen, B., Finnegan, N., Barling, N., Callahan, R.P., 2023. Symmetry in hillslope steepness and saprolite thickness between hillslopes with opposing aspects. *J. Geophys. Res. Earth Surf.* 128. <https://doi.org/10.1029/2023JF007076>.

Dworkin, S.I., Larson, G.J., Monaghan, G.W., 1985. Late Wisconsinan ice-flow reconstruction for the Central Great Lakes region. *Can. J. Earth Sci.* 22, 935–940.

Frederick, W.E., 1985. Soil Survey of Missaukee County. Government Printing Office, Michigan. U.S.

Godin, E., Fortier, D., 2012. Geomorphology of a thermo-erosion gully, Bylot Island, Nunavut, Canada. *Can. J. Earth Sci.* 49, 979–986.

Godin, E., Fortier, D., Coulombe, S., 2014. Effects of thermo-erosion gullyling on hydrologic flow networks, discharge and soil loss. *Environ. Res. Lett.* 9 (10), 105010.

Goudie, A.S., 2004. Encyclopedia of Geomorphology. Routledge, London.

GRASS Development Team., 2022. Geographic Resources Analysis support System (GRASS) software, Version 8.2. Open Source Geospatial Foundation. <https://grass.osgeo.org>. DOI: <https://doi.org/10.5281/zenodo.5176030>.

Hauber, E., Sassebroth, C., de Vera, J.P., Schmitz, N., Jaumann, R., Reiss, D., Hiesinger, H., Johnsson, A., 2019. Debris flows and water tracks in northern Victoria Land, continental East Antarctica: a new terrestrial analogue site for gullies and recurrent slope lineae on Mars. *Geol. Soc. Lond. Spec. Publ.* 467 (1), 267–287.

Heath, S.L., Loope, H.M., Curry, B.B., Lowell, T.V., 2018. Pattern of southern Laurentide Ice Sheet margin position changes during Heinrich Stadials 2 and 1. *Quat. Sci. Revs.* 201, 362–379.

Heinemann, G., 1999. The KABEG'97 Field experiment: an aircraft-based study of katabatic wind dynamics over the Greenland Ice Sheet. *Boundary Layer Meteor.* 93, 75–116.

Holmes, M.A., Syverson, K.M., 1997. Permafrost history of Eau Claire and Chippewa Counties, Wisconsin, as indicated by ice-wedge casts. *The Compass* 73, 91–96.

Hunkeler, R.V., Schaetzl, R.J., 1997. Spodosol development as affected by geomorphic aspect, Baraga County, Michigan. *Soil Sci. Soc. Am. J.* 61, 1105–1115.

Hupy, J.P., Aldrich, S., Schaetzl, R.J., Varnakovida, P., Arima, E., Bookout, J., Wangwang, N., Campos, A., McKnight, K., K., 2005. Mapping soils, vegetation, and landforms: an integrative physical geography field experience. *Prof. Geogr.* 57, 438–451.

Imhof, M., 1996. Modelling and verification of the permafrost distribution in the Bernese Alps (Western Switzerland). *Permafrost Periglac. Proc.* 7, 267–280.

Iwahana, G., Takano, S., Petrov, R.E., Shunsuke, T., Shingubara, R., Maximov, T.C., Fedorov, A.N., Desyatkin, A.R., Nikolaev, A.N., Desyatkin, R.V., Sugimoto, A., 2014. Geocryological characteristics of the upper permafrost in a tundra-forest transition of the Indigirka River Valley, Russia. *Polar Sci.* 8, 96–113.

Jacobs, P.M., Knox, J.C., Mason, J.A., 1997. Preservation and recognition of middle ad early Pleistocene loess in the Driftless Area, Wisconsin. *Quat. Res.* 47, 147–154.

Jasiewicz, J., Mickiewicz, A., 2023. Addon r.stream.slope. Geographic resources analysis support system (GRASS) software, version 8.2. <https://grass.osgeo.org/grass82/manuals/addons/r.stream.slope.html>.

Johnson, W.H., Hansel, A.K., Bettis III, E.A., Karrow, P.F., Larson, G.J., Lowell, T.V., Schneider, A.F., 1997. Late Quaternary temporal and event classifications, Great Lakes Region, North America. *Quatern. Res.* 47, 1–12.

Jorgenson, M.T., Osterkamp, T.E., 2005. Response of boreal ecosystems to varying modes of permafrost degradation. *Can. J. For. Res.* 35, 2100–2111.

Klatkowa, H., 1967. L'origine et les étapes d'évolution des vallées sèches et des vallons en berceau. Exemples des environs de Łódź. L'évolution des versants. Vol. 30, 167–174. Université Liège, Liège-Louvain.

Kokelj, A.V., Jorgenson, M.T., 2013. Advances in thermokarst research. *Permafrost Periglac. Proc.* 24, 108–119.

Langbein, W.B., 1964. Profiles of rivers of uniform discharge. U.S. Geol. Survey Prof. Paper 501B, 119–122.

Langohr, R., Sanders, J., 1985. The Belgium loess belt in the last 20,000 years: Evolution of soils and relief in the Zonien Forest. In: Boardman, J. (Ed.), Soils and Quaternary Landscape Evolution. Wiley, Chichester, UK, pp. 359–371.

Larson, G.J., Kincare, K., 2009. Late Quaternary history of the eastern mid-continent region, USA. In: Schaetzl, R.J., Darden, J.T., Brandt, D. (Eds.), Michigan Geography and Geology. Pearson Custom Publishing, Boston, MA, pp. 69–90.

Leigh, D.S., Knox, J.C., 1994. Loess of the Upper Mississippi Valley Driftless Area. *Quatern. Res.* 42, 30–40.

Leverett, F., Taylor, F.B., 1915. The Pleistocene of Indiana and Michigan and the history of the Great Lakes. U.S. Geological Survey Monograph 53. 529 pp.

Levy, J., 2015. A hydrological continuum in permafrost environments: the morphological signatures of melt-driven hydrology on Earth and Mars. *Geomorphology* 240, 70–82.

Lusch, D.P., Stanley, K.E., Schaetzl, R.J., Kendall, A.D., van Dam, R.L., Nielsen, A., Blumer, B.E., Hobbs, T.C., Archer, J.K., Holmstadt, J.L.F., May, C.L., 2009. Characterization and mapping of patterned ground in the Saginaw Lowlands, Michigan: possible evidence for late Wisconsin permafrost. *Annals Assoc. Am. Geog.* 99, 445–466.

Ma, Y., Zhang, Y., Zubrzycki, S., Guo, Y., Farhan, S.B., 2015. Hillslope-scale variability in seasonal frost depth and soil water content investigated by GPR on the southern margin of the sporadic permafrost zone on the Tibetan Plateau. *Permafrost Periglac. Proc.* 26, 321–344.

Malin, M., Edgett, K., 2000. Evidence for recent groundwater seepage and surface runoff on Mars. *Science* 288, 2330–2335.

Mann, D.H., Groves, P., Reanier, R.E., Kinz, M.L., 2010. Floodplains, permafrost, cottonwood trees, and peat: what happened the last time climate warmed suddenly in arctic Alaska? *Quat. Sci. Revs.* 29, 3812–3830.

Mason, J.A., 2015. Up in the refrigerator: Geomorphic response to periglacial environments in the Upper Mississippi River basin, USA. *Geomorphology* 248, 363–381.

Mason, J.A., Knox, J.C., 1997. Age of colluvium indicates accelerated late Wisconsinan hillslope erosion in the Upper Mississippi Valley. *Geology* 25, 267–270.

McKnight, D.M., Niyogi, D.K., Alger, A.S., Bomblies, A., Conovitz, P.A., Tate, C.M., 1999. Dry valley streams in Antarctica: Ecosystems waiting for water. *Bioscience* 49, 985–995.

McNamara, J.P., Kane, D.L., Hinzman, L.D., 1999. An analysis of an arctic channel network using a digital elevation model. *Geomorphology* 29, 339–353.

Nicu, I.C., Tanyas, H., Rubensdotter, L., Lombardo, L., 2022. A glimpse into the northernmost thermo-erosion gullies in Svalbard archipelago and their implications for Arctic cultural heritage. *Catena* 212. <https://doi.org/10.1016/j.catena.2022.106105>.

O'Callaghan, J.F., Mark, D.M., 1984. The extraction of drainage networks from digital elevation data. *Computer Vision, Graphics, and Image Proc.* 28, 323–344.

Panin, A.V., Fuzeina, J.N., Belyaev, V.R., 2009. Long-term development of Holocene and Pleistocene gullies in the Prota River basin, Central Russia. *Geomorphology* 108, 71–91.

Paquette, M., Fortier, D., Vincent, W.F., 2017. Water tracks in the High Arctic: a hydrological network dominated by rapid subsurface flow through patterned ground. *Arctic Sci.* 3, 334–353.

Paquette, M., Fortier, D., Vincent, W.F., 2018. Hillslope water tracks in the High Arctic: Seasonal flow dynamics with changing water sources in preferential flow paths. *Hydrolog. Proc.* 32, 1077–1089.

Patton, P.C., Schumm, S.A., 1975. Gully erosion, Northwestern Colorado: a threshold phenomenon. *Geology* 3, 88–90.

Poesen, J., Nachtergael, J., Verstraeten, G., Valentini, C., 2003. Gully erosion and environmental change: importance and research needs. *Catena* 50, 91–133.

Ponomarenko, E.V., Ershova, E.G., Stashenkov, D.A., Ponomarenko, D.S., Kochkina, A.F., 2020. Tracing land use history using a combination of soil charcoal and soil pollen analysis: an example from colluvial deposits of the Middle Volga Region. *J. Archaeol. Sci: Reports* 31, 102269.

Rowland, J.C., Jones, C.E., Altmann, G., Bryan, R., Crosby, B.T., Hinzman, L.D., Kane, D., Lawrence, D.M., Mancino, A., Marsh, P., McNamara, J.P., 2010. Arctic landscapes in transition: responses to thawing permafrost. *Eos, Transactions American Geophysical Union* 91, 229–230.

Rushlow, C.R., Godsey, S.E., 2017. Rainfall-runoff responses on Arctic hillslopes underlain by continuous permafrost, North Slope, Alaska. *USA. Hydrol. Proc.* 31, 4092–4106.

Rushlow, C.R., Sawyer, A.H., Voss, C.I., Godsey, S.E., 2020. The influence of snow cover, air temperature, and groundwater flow on the active-layer thermal regime of Arctic hillslopes drained by water tracks. *Hydrolog. J.* 28, 2057–2069.

Saeidi, T., Mosaddeghi, M.R., Afyuni, M., Ayoubi, S., Sauer, D., 2023. Modeling the effect of slope aspect on temporal variation of soil water content and matric potential using different approaches by HYDRUS-1D. *Geoderma Reg.* 35. <https://doi.org/10.1016/j.geodr.2023.e00724>.

Schaetzl, R.J., 2001. Late Pleistocene ice-flow directions and the age of glacial landscapes in northern lower Michigan. *Phys. Geog.* 22, 28–41.

Schaetzl, R.J., 2008. The distribution of silty soils in the Grayling Fingers region of Michigan: evidence for loess deposition onto frozen ground. *Geomorphology* 102, 287–296.

Schaetzl, R.J., Attig, J.W., 2013. The loess cover of northeastern Wisconsin. *Quatern. Res.* 79, 199–214.

Schaetzl, R.J., Weisenborn, B.N., 2004. The Grayling Fingers geomorphic region of Michigan: Soils, sedimentology, stratigraphy and geomorphic development. *Geomorphology* 61, 251–274.

Schaetzl, R.J., Enander, H., Luehmann, M.D., Lusch, D.P., Fish, C., Bigsby, M., Steigmeyer, M., Guasco, J., Forgacs, C., Polleyea, A., 2013. Mapping the physiography of Michigan using GIS. *Phys. Geog.* 34, 1–38.

Schaetzl, R.J., Lepper, K., Thomas, S.E., Grove, L., Treiber, E., Farmer, A., Fillmore, A., Lee, J., Dickerson, B., Alme, K., 2017. Kame deltas provide evidence for a new glacial lake and suggest early glacial retreat from central lower Michigan, USA. *Geomorphology* 280, 167–178.

Schaetzl, R.J., Baish, C., Colgan, P., Knauff, J., Bilintoh, T., Wanyama, D., Church, M., McKeahan, K., Fulton, A., Arbogast, A.F., 2020. A sediment-mixing process model of till genesis, using texture and clay mineralogy data from Saginaw Lobe (Michigan, USA) tills. *Quatern. Res.* 94, 174–194.

Schaetzl, R.J., Running IV, G., Larson, P., Rittenour, T., Yansa, C., Faulkner, D., 2021. Luminescence dating of sand wedges constrains the late Wisconsin (MIS-2) permafrost interval in the Upper Midwest, USA. *Boreas* 50. <https://doi.org/10.1111/bor.12550> 17 pp.

Schaetzl, R.J., Miller, B.A., Baish, C., 2021a. Catenas and Soils. In: *Treatise on Geomorphology*, 2nd ed., Vol. 4. J.F. Shroder (ed.). Academic Press, San Diego, CA. doi:<https://doi.org/10.1016/B978-0-12-818234-5.00214-5> 15 pp.

Schumm, S.A., 1979. Geomorphic thresholds: the concept and its applications. *Trans. Inst. British Geog.* 4, 485–515.

Sidorchuk, A., 1999. Dynamic and static models of gully erosion. *Catena* 37, 401–414.

Sidorchuk, A., 2020. The potential of gully erosion on the Yamal peninsula, West Siberia. *Sustainability* 12, 260.

Sidorchuk, A.Y., Golosov, V.N., 2003. Erosion and sedimentation on the Russian Plain, II: the history of erosion and sedimentation during the period of intensive agriculture. *Hydrol. Proc.* 17, 3347–3358.

Soms, J., 2011. Development and morphology of gullies in the river Daugava Valley. South-Eastern Latvia. *Landform Anal.* 17, 183–192.

Spell, R.L., Johnson, B.G., 2019. Anthropogenic alluvial sediments in North Carolina Piedmont gullies indicate swift geomorphic response to 18th century land-use practices. *Phys. Geogr.* 40 (6), 521–537.

Tardy, S.W., 2005. Soil Survey of Roscommon County. Government Printing Office, Michigan, U.S.

Tebebu, T.Y., Abiy, A.Z., Zegeye, A.D., Dahlke, H.E., Easton, Z.M., Tilahun, S.A., Collick, A.S., Kidnau, S., Moges, S., Dadgari, F., Steenhuis, T.S., 2010. Surface and subsurface flow effect on permanent gully formation and upland erosion near Lake Tana in the northern highlands of Ethiopia. *Hydrol. Earth System Sci.* 14, 2207–2217.

Thwaites, R.N., Brooks, A.P., Pietsch, T.J., Spencer, J.R., 2022. What type of gully is that? The need for a classification of gullies. *Earth Surf. Process. Landf.* 47 (1), 109–128.

Torri, D., Poesen, J., 2014. A review of topographic threshold conditions for gully head development in different environments. *Earth-Science Revs.* 130, 73–85.

Trochim, E.D., Jorgenson, M.T., Prakash, A., Kane, D.L., 2016. Geomorphic and biophysical factors affecting water tracks in northern Alaska. *Earth Space Sci.* 3, 123–141.

Tsuyuzaki, S., Ishizaki, T., Sato, T., 2001. Vegetation Structure in Gullies Developed by the Melting of Ice Wedges along Kolyma River, Northern Siberia. *Research, Ecol.* <https://doi.org/10.1046/j.1440-1703.1999.00316.x>.

Vader, M.J., Zeman, B.K., Schaetzl, R.J., Anderson, K.L., Walquist, R.W., Freiberger, K. M., Emmendorfer, J.A., Wang, H., 2012. Proxy evidence for easterly winds in Glacial Lake Algonquin, from the Black River Delta in northern lower Michigan. *Phys. Geogr.* 33, 252–268.

Valentin, C., Poesen, J., Li, Y., 2005. Gully erosion: Impacts, factors and control. *Catena* 63, 132–153.

Vandaele, K., Poesen, J., Govers, G., van Wesemael, B., 1996. Geomorphic threshold conditions for ephemeral gully incision. *Geomorphology* 16, 161–173.

Warntz, W., 1975. Stream ordering and contour mapping. *J. Hydrol.* 25, 209–227.

Werlein, J.O., 1998. *Soil Survey of Crawford County*. Government Printing Office, Michigan, U.S.

Wilkinson, K.N., 2003. Colluvial deposits in dry valleys of southern England as proxy indicators of paleoenvironmental and land-use change. *Geoarchaeol* 18, 725–755.

Zachar, D., 2011. Soil erosion. Elsevier. 544 pp.

Zglobicki, W., Poesen, J., Cohen, M., Del Monte, M., García-Ruiz, J.M., Ionita, I., Niacsu, L., Machová, Z., Martín-Duque, J.F., Nadal-Romero, E., Pica, A., 2019. The potential of permanent gullies in Europe as geomorphosites. *Geoheritage* 11, 217–239.

Zwieback, S., 2021. Topographic asymmetry across the Arctic. *Geophys. Res. Letters* 48. doi:<https://doi.org/10.1029/2021GL094895>.